

EFFECTS OF VARIABLE STABILITY IN A 1000-MB. GRAPHICAL PREDICTION MODEL

DALE A. LOWRY

Techniques Development Laboratory, Weather Bureau, ESSA, Silver Spring, Md.

EDWIN F. DANIELSEN¹

Department of Meteorology, The Pennsylvania State University, University Park, Pa

ABSTRACT

The most striking shortcomings of previous 1000-mb. forecast models have been over-intensification of pressure systems, especially anticyclones, and inferior predictions in and near mountains. In this article a graphical-numerical two-level prediction model that incorporates a variable mean stability is developed and tested. When the mean stability is small, the 1000-mb. prediction is determined primarily by the 500-mb. steering and height changes. As the stability increases the 500-mb. control decreases and the effective mountain wind exerts more control over the 1000-mb. changes. Since the stability is generally larger in anticyclones than cyclones the anticyclones are steered by a smaller percentage of the 500-mb. wind and are more influenced by the mountain topography.

Twenty-four-hour forecasts were handproduced daily for the month of September 1965. Predictions were also prepared using a constant stability model, and the forecasts of the two models were compared statistically by rigorous verification techniques. It was found that a definite improvement in the overall product can be expected by application of the variable stability model as opposed to the constant stability technique, especially in the mountainous areas and around anticyclones.

1. INTRODUCTION

Various numerical graphical models have been produced in recent years to predict the future pressure patterns and intensities at 1000 mb. In most cases the models have been simplified by holding coefficients constant and assigning them average values. These simplifications have allowed liberal use of the techniques, but have also produced certain systematic errors. The most striking errors have been over-intensification of pressure systems, especially anticyclones, and inferior predictions in and near mountain regions. The purpose of this study is to allow for variable coefficients in a forecast equation by permitting stability to vary and to determine if the results produce a significant improvement over existing constant static stability techniques.

Pioneer research by Fjørtoft [8] provided the first purely graphical approach to the problem of integrating the vorticity equation. Considerable success was obtained in the determination of 500-mb. height changes under the barotropic assumption. This assumption provided that the motion at levels close to the 500-mb. level was horizontal and nondivergent; thus absolute vorticity was conserved.

The Fjørtoft method was expanded by Estoque [5] to a simple baroclinic model which predicted cyclone development at the earth's surface. Surface vorticity advection by the surface wind, and also by the wind at the level of nondivergence, was assumed to be small. In effect, the

advection of the surface vorticity by the thermal wind was not included.

The following year Estoque [6] generalized his earlier work and introduced a model that did include the advection of surface vorticity by the thermal wind. A sinusoidal profile of vertical velocity was utilized. At the same time Reed [14] introduced a model similar to Estoque's later model; except in place of a sinusoidal vertical velocity profile, he used a simplified linear relationship.

Following development of the basic techniques, modifications were considered by several authors. Orographic effects were studied by Estoque [7] and later by Haltiner and Hesse [9]. Nonadiabatic heating effects, along with the mountain term, were studied by Reed [15] and again by Haltiner and Wang [10]. The findings of these studies revealed that improved 1000-mb. or surface forecasts could be expected by the introduction of modifications to the simple basic models. The desirability of obtaining a better estimate of the coefficients, especially for displacing surface pressure systems with the upper flow and reflecting down the 500-mb. height changes, was pointed out by Reed [16].

The graphical process was adapted for computer solution by Reed [17] at the National Meteorological Center (NMC) in Suitland, Md. A parabolic vertical velocity profile, similar to that suggested by Sawyer and Bushby [18], was used in the constant stability model to replace the linear relationship used in his previous work. Much preliminary experimentation was required to determine the merits of a strictly Eulerian approach as opposed to a quasi-Lagrangian forecast method. The quasi-Lagrangian program yielded superior results and was integrated into

¹ Present affiliation: Department of Geosciences, University of Hawaii, Honolulu, Hawaii.

the operational NMC workload. Coefficients were altered on the basis of empirical experience, and a mountain term was included. Also, the mesh length used was 775 km. which is approximately twice the standard NMC operational grid distance of 381 km. at 60°N. Aside from the manner in which the forecast equations have been solved, the primary difference between the Reed [17] model and the model presented in this study is the handling of the stability factor.

Recent independent studies have shown that improvements are possible through variation of coefficients, different methods of solution, and by further modifications. Muench [13] computed coefficients that varied with latitude and categorically with 500-mb. height rises and falls. Jarvis [11] designed a grid method to solve the forecast equation and compared the results for cyclones with those obtained by Veigas and Ostby [20] who used regression equation prediction. Danard [2] [3] [4] provided information that led to the inclusion of latent heat liberation in a quasi-geostrophic numerical model. The results indicated that the latent heat factor contributed a measurable portion of the 1000-mb. height change that was previously unexplained.

The method of numerical solution used in this study is not unique. Three equations are used in the two-level (500 and 1000 mb.) model: the vorticity equation, the continuity equation, and the energy equation. The divergence can be eliminated by use of the continuity equation but the vorticity equation applied at 1000 mb. still contains two unknowns (height and vertical velocity). The vertical velocity can be eliminated by using the energy equation that leads to a single prediction equation with one unknown (height).

In general, the various graphical models referenced contain several assumptions in common and a few that are unique to the particular model. Described here are the assumptions of the 1000-mb. forecast model used in this study.

1) The motion is assumed to be geostrophic, hydrostatic, and adiabatic. These are only fair assumptions. Ageostrophic effects, although small at the 500-mb. level, were shown by Muench [13] to be considerable at 1000 mb. Also, diabatic heat sources as outlined by Haltiner and Wang [10] are undoubtedly important for forecasting 1000-mb. height changes. Reed [15] reported favorable results when a nonadiabatic heat factor was added to the Gulf of Alaska area. Danard [2] [3] [4] found that the liberation of latent heat was a key factor in explaining pressure changes at the earth's surface.

2) A linear divergence profile in the vertical, a straight wind hodograph, and a parabolic vertical velocity profile are assumed. These are consistent first approximations.

3) The tilting term and the vertical advection of relative vorticity term in the vorticity equation are assumed small and neglected. These are excellent assumptions at 1000 mb. over level terrain where the vertical velocity is usually either small or nonexistent.

4) Friction is assumed to be small and is not included. Although it is not considered a problem at 500 mb. since that level is well above the friction layer, at 1000 mb. the neglect of friction may contribute a sizable error.

5) The 500-mb. level is assumed to be near the level of nondivergence and the 1000-mb. level is assumed to be near the level of maximum divergence. Experience has shown that any error in the final product introduced as a result of these assumptions is small.

2. THEORY

This particular model for operational use requires that 500-mb. heights and temperatures as well as surface temperature prognoses be readily available. If this is not the case, Lowry [12] has outlined a detailed graphical procedure based on the findings of Fjørtoft [8] and the Air Weather Service [1] that produces forecasts of the needed variables.

In the derivation of the 1000-mb. prediction model the simplified vorticity equation applied to the 1000-mb. level is

$$\frac{\partial \zeta_0}{\partial t} = -\mathbf{V}_0 \cdot \nabla f(\zeta_0 + f) + f \left(\frac{\partial \omega}{\partial p} \right)_0, \quad (1)$$

where ζ is the vertical component of the relative vorticity, \mathbf{V} the horizontal geostrophic wind velocity, f the Coriolis parameter, ω the total rate of change of pressure, and p the pressure. ∇ is the del operator, t is time, and the subscript 0 refers to the 1000-mb. level. In equation (1) the continuity equation has been used to eliminate the divergence and its coefficient has been reduced by neglecting ζ_0 relative to f .

Following the theory outlined by Reed [17] we express equation (1) in terms of height (z) as

$$\frac{\partial}{\partial t} (\bar{z}_0 - z_0) = -\mathbf{V}_0 \cdot \nabla (\bar{z}_0 - z_0 + G) + f/a \left(\frac{\partial \omega}{\partial p} \right)_0 \quad (2)$$

where

$$\zeta_0 \approx a(\bar{z}_0 - z_0), \quad (3)$$

$$a = \frac{4gm^2}{fd^2}, \quad (4)$$

and

$$\nabla G = \frac{1}{a} \nabla f. \quad (5)$$

In equation (2) the relative vorticity has been approximated by the geostrophic vorticity and then reduced to the finite difference form of equation (3) by neglect of the variation of f . The proportionality constant, a , includes the acceleration of gravity, g , the mapping factor, m , a mean value of f , and the grid distance, d . The grid distance is important because it determines the scale of the vorticity resolved by the finite difference approximation.

We obtain a second equation in z and ω from the energy equation by assuming adiabatic motions and introducing

the hydrostatic approximation. Integration between 1000 and 500 mb. leads to

$$\frac{\partial}{\partial t}(z_5 - z_0) + \mathbf{V}_0 \cdot \nabla(z_5 - z_0) - \sigma p_5 \bar{\omega} = 0 \quad (6)$$

under the assumption that the geostrophic wind varies linearly with pressure. The subscript 5 refers to the 500-mb. level. In equation (6) the stability, σ , should be an ω weighted mean but in practice an unweighted mean is used with

$$\sigma = -\frac{\alpha}{g\theta} \frac{\partial \theta}{\partial p} \quad (7)$$

In equation (7) θ is potential temperature and α is specific volume.

To eliminate $\partial \omega / \partial p$ from equation (2) and $\bar{\omega}$ from equation (6) we assume also that the horizontal divergence at constant pressure varies linearly with pressure. Integration with respect to pressure then gives

$$\left(\frac{\partial \omega}{\partial p} \right)_0 = -\frac{2(\omega_5 - \omega_0)}{p_5} \quad (8)$$

and

$$\bar{\omega} = \frac{2}{3} \left(\omega_5 + \frac{\omega_0}{2} \right) \quad (9)$$

In addition, we relate ω_0 to the 1000-mb. wind and the earth's topography by assuming

$$\omega_0 = -\mathbf{V}_0 \cdot \nabla(p_0 - p_{sfc}) \quad (10)$$

where p_{sfc} is the standard pressure at the earth's surface.

From equations (2), (6), (8), (9), and (10) we obtain

$$\begin{aligned} \frac{\partial z_0}{\partial t} = & -\frac{1}{1+k} \left[\mathbf{V}_0 \cdot \nabla(z_0 - \bar{z}_0) + \mathbf{V}_0 \cdot \nabla G + \frac{\partial \bar{z}_0}{\partial t} + \mathbf{V}_0 \cdot \nabla z_m \right] \\ & + \frac{k}{1+k} \left[\mathbf{V}_0 \cdot \nabla(z_5 - z_0) + \frac{\partial z_5}{\partial t} \right] \end{aligned} \quad (11)$$

where

$$k = \frac{3\bar{f}}{a\sigma p_5^2} \quad (12)$$

and

$$z_m = \frac{3\bar{f}}{a p_5} (p_0 - p_{sfc}). \quad (13)$$

Finally, recognizing that under the geostrophic approximation

$$\mathbf{V}_0 \cdot \nabla z_0 = 0$$

and

$$\mathbf{V}_0 \cdot \nabla z_5 = -\mathbf{V}_5 \cdot \nabla z_0,$$

we obtain the prediction equation

$$\begin{aligned} \frac{\partial z_0}{\partial t} = & -\left[\frac{\bar{\mathbf{V}}_0 - \mathbf{V}_G + \mathbf{V}_m}{1+k} + \frac{k}{1+k} \mathbf{V}_5 \right] \cdot \nabla z_0 \\ & + \frac{1}{1+k} \frac{\partial \bar{z}_0}{\partial t} + \frac{k}{1+k} \frac{\partial z_5}{\partial t} \end{aligned} \quad (14)$$

The mesh length d was chosen as six degrees of latitude at 60°N. With a grid distance this large the advections by $\bar{\mathbf{V}}_0$ and \mathbf{V}_G can be neglected relative to the advections by \mathbf{V}_m and \mathbf{V}_5 . Neglecting the $\bar{\mathbf{V}}_0$ term in and near cold anticyclones may not be a good assumption, but since a relaxation process is indicated it becomes impracticable to include this term in a graphical procedure. Also, neglecting $\partial \bar{z}_0 / \partial t$ relative to $\partial z_5 / \partial t$ leads to the final forecast equation

$$\frac{\partial z_0}{\partial t} = -\left(\frac{\mathbf{V}_m}{1+k} + \frac{k}{1+k} \mathbf{V}_5 \right) \cdot \nabla z_0 + \frac{k}{1+k} \frac{\partial z_5}{\partial t} \quad (15)$$

The theory indicates that k varies inversely with stability. It can be seen from equation (15) that when stability is large ($k \rightarrow 0$) the local change is produced primarily by the effective mountain wind. Conversely, when the stability is small ($k \rightarrow \infty$) the local change is produced primarily by the 500-mb. advection and 500-mb. height change.

In general, larger values of stability are associated with anticyclones, while smaller values are associated with cyclones. Therefore, cyclones will generally travel faster and be less affected by the mountains than anticyclones.

3. PROCEDURE

Graphical solutions of the forecast equations were computed over an area consisting mostly of North America plus portions of the adjoining oceanic regions (see figure 1). Twenty-four-hour predictions were obtained by using a single time step. Preliminary experimentation showed that shorter time steps would have been more desirable but impracticable without the use of high-speed computers.

The Lambert conformal conic map projection, true at 30° and 60°, was chosen to minimize the variation in the map scale factor (m) which was then considered to be unity. A one to 10 million map scale was used.

Preliminary testing utilized only initial synoptic data from the typically weak-gradient case of 0000 GMT, June 9, 1964. Each step of the detailed graphical forecast procedure devised by Lowry [12] was carried to completion. The procedure yields forecasts of 500-mb. heights and temperatures in addition to surface temperature and sea level pressure. Results indicated that the method was workable with a minimum amount of initial data. Initial contours and isotherms at 500 mb. plus isotherms at the earth's surface and isobars at the surface, reduced to sea level, were required. The latter data were quickly converted to 1000-mb. contours by use of surface to 1000-mb. height conversion tables. Surface isotherms were used directly as 1000-mb. data, which amounts to an isothermal assumption in the lowermost layer.

Final testing was made once per day (forecasts verified at 1200 GMT) for the month of September 1965. September was chosen as being a month that would normally produce moderate or near average gradients of pressure and temperature. The modified graphical procedure outlined by Lowry [12] was used for the 1-month test to produce

1000-mb. forecasts. The modified procedure differs from the detailed procedure in only one fashion. It allows certain observed data to be used in place of prognostic material for study purposes. In this study observed 500.-mb. contours and isotherms and surface isotherms were used.

To isolate the effects of stability a comparison was made between the variable stability model, equation (15), and one of the uniform stability models. The simplest model is obtained by setting $k=1.00$. Equation (15) reduces to

$$\frac{\partial z_0}{\partial t} = -\frac{1}{2} (\mathbf{V}_m + \mathbf{V}_s) \cdot \nabla z_0 + \frac{1}{2} \frac{\partial z_s}{\partial t} \quad (16)$$

and will be referred to as the constant stability model. In words, the 1000-mb. heights are advected by one-half the 500-mb. geostrophic wind and one-half the geostrophic wind determined by the effective height of the mountains. The results are added to one-half the 500-mb. height change to produce the 1000-mb. prognosis. The mountain term, sometimes neglected, was retained here because of its close relationship to k and σ .

In (7), if the derivative is replaced by a finite difference, then

$$\sigma \approx \frac{\alpha}{g\theta p_5} \Delta\theta \quad (17)$$

where $\Delta\theta$ is $\theta_s - \theta_0$. Experience has shown that $\alpha/(g\theta p_5)$ is nearly constant at $0.074 \times 10^{-7} \text{ gm.}^{-2} \text{ cm.}^3 \text{ sec.}^4$. The relationship between k and σ shown in (12) reveals that k is inversely proportional to σ where the α defined by (4) is the absolute constant $8.81 \times 10^{-9} \text{ cm.}^{-1} \text{ sec.}^{-1}$ and the quantity.

$$\frac{3\bar{f}}{ap_5^2} = 1.36 \times 10^{-7} \text{ gm.}^{-2} \text{ cm.}^3 \text{ sec.}^4 = \sigma k. \quad (18)$$

TABLE 1.—Coefficient conversions used to facilitate graphical computations. The $\Delta\theta$ of 18.4 is shown since it corresponds to a k of 1.00, the value used in the constant stability comparison model. $\Delta\theta$ values in $^{\circ}\text{A.}$, σ values in $10^{-7} \text{ gm.}^{-2} \text{ cm.}^3 \text{ sec.}^4$

| $\Delta\theta$ | σ | k | $\frac{1}{1+k}$ | $\frac{k}{1+k}$ |
|----------------|----------|------|-----------------|-----------------|
| 5 | .37 | 3.68 | .21 | .79 |
| 10 | .74 | 1.84 | .35 | .65 |
| 15 | 1.11 | 1.23 | .45 | .55 |
| 18.4 | 1.36 | 1.00 | .50 | .50 |
| 20 | 1.48 | .92 | .52 | .48 |
| 25 | 1.85 | .74 | .57 | .43 |
| 30 | 2.22 | .61 | .62 | .38 |
| 35 | 2.59 | .53 | .65 | .35 |
| 40 | 2.96 | .46 | .68 | .32 |
| 45 | 3.33 | .41 | .71 | .29 |
| 50 | 3.70 | .37 | .73 | .27 |
| 55 | 4.07 | .33 | .75 | .25 |

TABLE 2.—Effective height of mountains (z_m)

| Mountain height (ft.) | Average surface pressure (mb.) | Effective height (m.) |
|-----------------------|--------------------------------|-----------------------|
| 0 | 1000 | 0.0 |
| 2000 | 940 | 40.9 |
| 4000 | 874 | 85.8 |
| 6000 | 810 | 129.4 |
| 8000 | 752 | 168.9 |

For the special constant stability case where $k=1.00$, $\sigma=1.36 \times 10^{-7} \text{ gm.}^{-2} \text{ cm.}^3 \text{ sec.}^4$ and the corresponding $\Delta\theta$ is 18.4°A. These values, computed from (17) and (18), can be found in table 1 along with other combinations of $\Delta\theta$, σ , k , $1/(1+k)$, and $k/(1+k)$.

The effective heights of the mountains were computed for 2000-ft. intervals according to (13) and the results listed in table 2. The average surface pressures were used for the given elevations.

An ordinary smoothed elevation map (see figure 1) was converted into an effective height (z_m) chart. Although the effective heights do not change, it should be noted that the resulting wind component \mathbf{V}_m is allowed to be weighted according to $1/(1+k)$. A smoothed terrain was employed primarily because a ragged terrain is extremely difficult to handle graphically.

4. RESULTS AND DISCUSSION

Comparative verification was made using the operational NMC 49-point grid (see figure 2). This represents a major portion of the nonoperational NMC 63-point grid that is a rectangle having outer boundaries of 55°N. , 25°N. , 65°W. , and 145°W. Increments used are 5° of latitude and 10° of longitude. Forecast and observed pressure values to the nearest millibar were extracted at each point daily.

The particular score used is the operational NMC S_1 score devised by Teweles and Wobus [19] that is a measure of the gradient forecasting skill and has been used continuously for approximately 20 yr. By definition

$$S_1 = \sum_i \frac{|e|}{|G|} (100)$$

where e is the error in gradient between two points (the

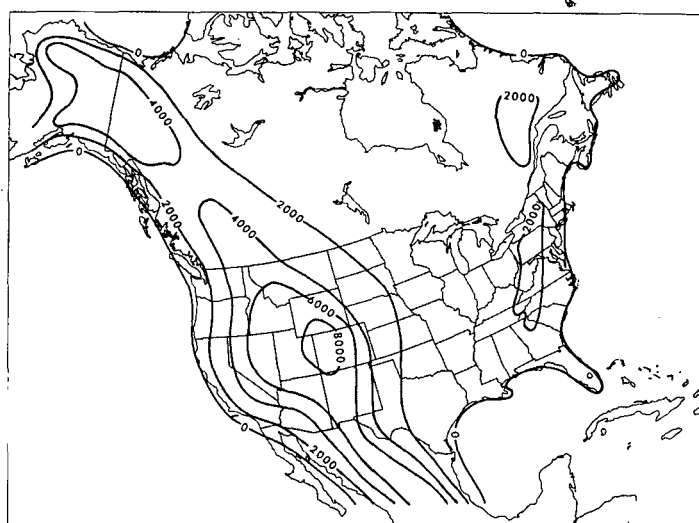


FIGURE 1.—The approximate initial data coverage area. The valid prediction area is somewhat smaller because of boundary conditions. Also, the smoothed elevation contours used to define the effective height field are shown in feet.

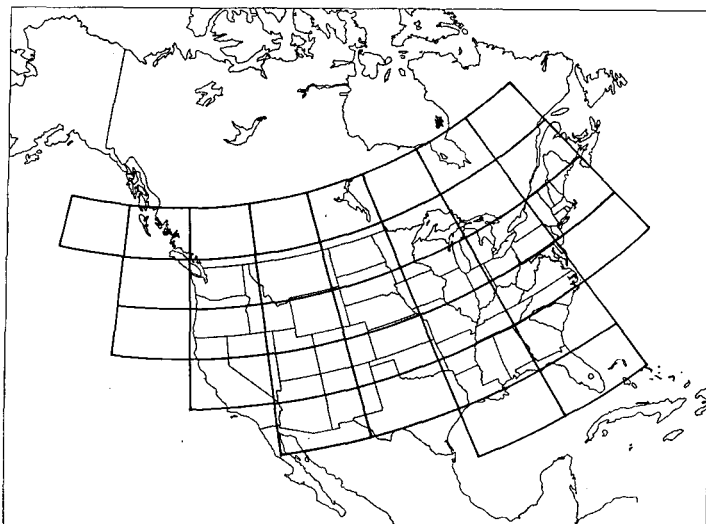


FIGURE 2.—Intersections represent the operational NMC 49-point grid used for comparative verification. Increments used are 5° of latitude and 10° of longitude.

TABLE 3.—Monthly average verification comparisons of 24-hr. forecasts

| | Constant Stability | Variable Stability |
|--|--------------------|--------------------|
| Grid Point Comparisons | | |
| 1. S_1 score (gradient skill)..... | 63 | 61 |
| 2. Root mean square error (mb.)..... | 4.54 | 4.42 |
| 3. Mean absolute error (mb.)..... | 3.40 | 3.29 |
| Moving System Comparisons | | |
| 1. Pressure error of anticyclones (mb.)..... | +2.00 | +1.12 |
| 2. Distance error of anticyclones (n.mi.)..... | 227 | 225 |
| 3. Pressure error of cyclones (mb.)..... | -1.00 | +0.18 |
| 4. Distance error of cyclones (n.mi.)..... | 211 | 245 |

difference between the gradient forecast and that observed), G is the forecast gradient or the observed gradient (whichever is larger), and i is the number of individual grid point pairs used (both E-W and N-S). In this case $i=82$. A perfect prognosis would have no error in gradient and would score zero while the worst possible prediction could be no worse than 200.

Table 3 shows the average S_1 scores for the month of September 1965 under both constant and variable stability conditions. The range of scores turned out to be from the low fifties to the middle seventies, with averages in the low sixties. This indicates a certain degree of skill in both products since a score of 100 would show no skill.

To determine from the 30-day sample if a significant improvement over the constant stability model could be expected by using the variable stability model, the standard paired t test was used. This test can only be used for dependent (matched) samples. Since the results shown here are for the same days the pairs are matched synoptically. The formula used is

$$t = \frac{\bar{D} \sqrt{N(N-1)}}{[\sum D_i^2 - N\bar{D}^2]^{1/2}}$$

where \bar{D} is the mean difference of the pairs for the sample, N is the number of cases in the sample, and D_i is the individual difference of the pairs within the sample. The resulting t value was 1.99. This figure was converted to probable significance using standard two-tailed t test

tables. The improvement shown by the variable stability model over the constant stability model was shown to be significant at the 10-percent level. If we use 29 degrees of freedom with 30 cases we also assume that the individual cases, or days, are independent of each other. Since weather has a regime tendency this is not a valid assumption. However, close inspection of the degrees of freedom in relation to the probability limits reveals that even if the degrees of freedom were reduced to 6, significance would still be indicated at the 10-percent level. The correct number (degrees of freedom) is not known without a complex regime index but would certainly fall somewhere between the values of 29 and 6.

Table 3 also shows the monthly averages for two other grid point comparisons. The two, root mean square error and mean absolute error, showed a favorable but not significant improvement when stability was varied.

Centers of cyclones and anticyclones sometimes have a peculiar knack of eluding verification grid points. Therefore the characteristics of the pressure systems were studied individually. During the month there were 155 cyclones and 131 anticyclones, an average of about five cyclones and four anticyclones per map.

The cyclones were found to move faster in the constant model. In fact, of 155 cases, only three cyclones forecast by the variable model moved faster and in all three cases this was an improvement. Constant model cyclones were also found to be deeper than variable model cyclones. Only 17 of 155 cyclones were predicted to have a lower central pressure by the variable stability model. In nine cases the lower pressures represented an improvement. Five of the remaining eight cases had a smaller distance error.

Anticyclones were also forecast to move faster by the constant model. Four variable model anticyclones in a group of 131 moved faster and in all four cases this was an improvement. Central pressures of anticyclones produced by the constant model proved to be higher. Nine of the 131 anticyclones were higher in the variable model, of which five were better and four were worse. Of the four that were worse, with respect to central pressure, three had a smaller distance error than the constant model anticyclones.

Further study and comparative verification (see table 3) was made in a category called "moving systems." All pressure centers were eliminated that could be classified as either stationary or tropical, or could not be identified on both forecasts and the observed chart. The remaining 49 anticyclones and 33 cyclones were subjected to central pressure error tests and distance error tests.

The center values of the anticyclones in the constant stability model were found to have an average error of +2.00 mb. while the variable model showed a +1.12-mb. error. The difference produced a paired $t=2.90$ that indicates a reduction in the central pressure of moving anticyclones by the variable model that is significant at the 1 percent level (if we assume at least 17 degrees of freedom). This amounts to a large improvement since both were forecast too high. The average 24-hr. distance error of the central pressures in the constant model was

227 n.mi. while the variable model was slightly better at 225 n.mi.

Cyclones forecast by the constant model yielded central values that had an average error of -1.00 mb. (too deep) while the variable model showed a $+0.18$ -mb. error (see table 3). The difference produced a paired $t=2.24$ that indicates a higher central pressure of moving cyclones by the variable model that is significant at the 5 percent level (if we allow at least 10 degrees of freedom). Most of this increase was improvement since the variable model forecast too high only slightly. The average 24 hr. central pressure distance error of the constant model was 211 n.mi. while the variable model gave 245 n.mi. The difference produced a paired $t=2.14$ which means the distance error improvement of the constant model over the variable model is significant at the 5 percent level (if we permit at least 15 degrees of freedom).

Any comparative verification scheme is difficult because no single set of figures can adequately describe the product. Several types of verification have been used here in an attempt to overcome this barrier.

Equally as difficult is the problem of isolating error producing terms of the forecast equations in specific cases. All prognostic features are combinations of weighted advecting and deepening terms. For this reason the products here have been subjected to a "complete map" test as opposed to "single system" approach.

Some charts showed a tendency to split a single system into two parts. This is probably because a single time step was used for a 24-hr. period, and shorter intervals would have helped eliminate that problem. Specific examples were observed during the test period with respect to hurricanes over water where the upper-level contours were analyzed parallel to the lower-level contours. No advective movement is possible under these conditions and the storms were forecast to be stationary. However, other predicted depressions appeared nearby directly under the upper-level height falls as a product of the deepening term. Thus hurricanes with two centers were forecast in error by both models tested.

The observed σ field agreed very well with the theory that, in general, larger values of stability are associated with anticyclones while smaller values are associated with cyclones. There was also a tendency for the centers of low stability to shift toward the upper-level cold air.

The k field showed an interesting range from 1.23 to 0.37 isolines. Only seven cases produced k values over 1.00 which was the k used in the constant stability model. The $k=1.00$ value is good with respect to the speed of movement of deep cyclones and troughs away from the mountains. It is for this reason, in addition to the simplicity factor, that the $k=1.00$ value was chosen for use here. For the few cases where the observed k exceeded 1.00 the variable model systems moved faster and were more intense than constant model systems, in agreement with the theory. Also, in agreement with the k theory, the variable model cyclones generally moved faster and were less affected by the mountains than anticyclones.

Large errors in the constant model seemed to appear as false gradients that were too strong between anticyclones,

which were forecast too high, and cyclones, which were forecast too deep. The variable model produced gradients that were much more realistic by reducing the over-intensification tendencies, especially around anticyclones, of the constant model.

Predictions in mountainous areas did benefit greatly by the weighted advecting mountain term of the variable stability model. It would seem that when large k values are not found over the mountains that all variable model systems would move more slowly than constant model systems. This is not always the case because strongly weighted mountain flow can become stronger than weakly weighted 500-mb. flow (high σ , $k \rightarrow 0$).

It is possible that a constant k different from 1.00 exists that could be considered an optimum value. However, any different constant model k value should tend to shift the errors synoptically and seasonally rather than correct them. For example, a constant stability model where $k=0.50$ should produce very large errors near cyclones where the observed k is considerably higher. Also, these errors should be greatly magnified in mountainous areas because of the weighting factors. Different seasons of the year would probably produce different optimum k values. Reed [17] at NMC used a constant k of 1.22 regardless of the season. Experience has shown the best average constant stability value of k to be near 1.00, which is the value used in this study for comparison purposes.

Many of the characteristics mentioned here can be observed in the five selected forecast cases shown (see figures 3 to 27). These selected forecasts correspond to initial data times of 1200 GMT on September 1, 4, 11, 15, and 17, 1965. In each instance the valid prediction period is 24 hr. Five illustrations are used to represent each case. These include initial sea level pressure, initial k distribution, constant stability forecast, variable stability forecast, and the observed 24-hr. sea level pressure. Each of the five cases is discussed individually with respect to distance, central pressure, and pressure gradient errors forecast by the two models. Fronts are excluded from the study.

The typical synoptic distribution of k can be noted in all cases; low values of k (high stability) are associated with anticyclones and high values of k (low stability) are associated with cyclones. The slopes of the synoptic systems with height can be shown rather well by the stability field once the relationship has been established. It can also be noted that observed values of k near cyclones during the test period were usually found to be something less than 1.00, the value used in the constant model, and the k values observed near anticyclones were usually found to be about 0.50 or one-half the value used in the constant model.

A close look at the daily forecasts of cyclone positions shows that in and near mountains the variable model is actually better (see the first case as an example) and away from the mountains the constant model is better (this can also be seen in the first case over eastern Canada). Considering the magnitude of the errors and the fact that nonmountainous terrain is predominant, the constant model forecast cyclone positions better on the monthly average.

FIRST CASE

The initial conditions (fig. 3) reveal a pair of 1006-mb. cyclones in southern Canada plus an anticyclone over Kansas on September 1, 1965. The observed values of k (fig. 4) show a typical relationship to the synoptic patterns. The 24-hr. 1000-mb. forecasts converted to sea level pressure (figs. 5 and 6) and the observed sea level pressure analysis (fig. 7) show several interesting features. The forecast cyclone in South Central Canada shows the variable model central pressure to be better by 4 mb. and the position is also better, evidently because of the weighted mountain term. The anticyclone over-intensification by the constant model was entirely removed by the variable model and the distance error is about the same. The eastern Canadian cyclone and trough show the forecast pressure to be better by the variable model and the position, or distance, to be better by the constant model. All of the features discussed on the first case may be termed as typical.

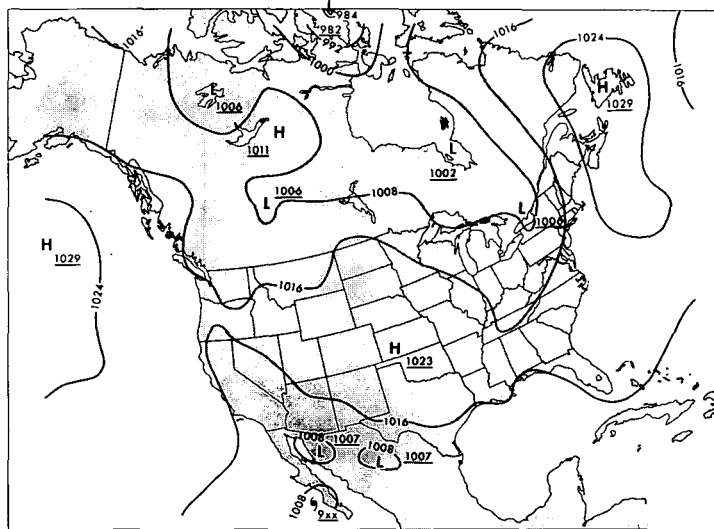


FIGURE 3.—Initial synoptic sea level pressure analysis in millibars for 1200 GMT, Sept. 1, 1965. Central values are underlined.

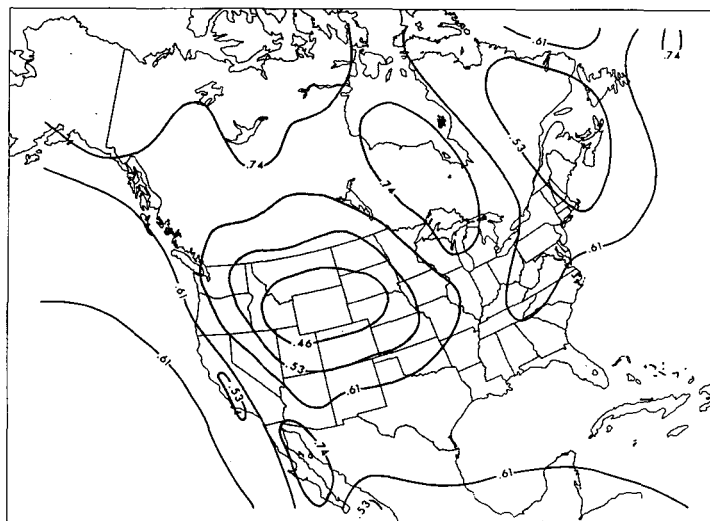


FIGURE 4.—Initial synoptic k values for 1200 GMT, Sept. 1, 1965. Low k indicates high static stability.

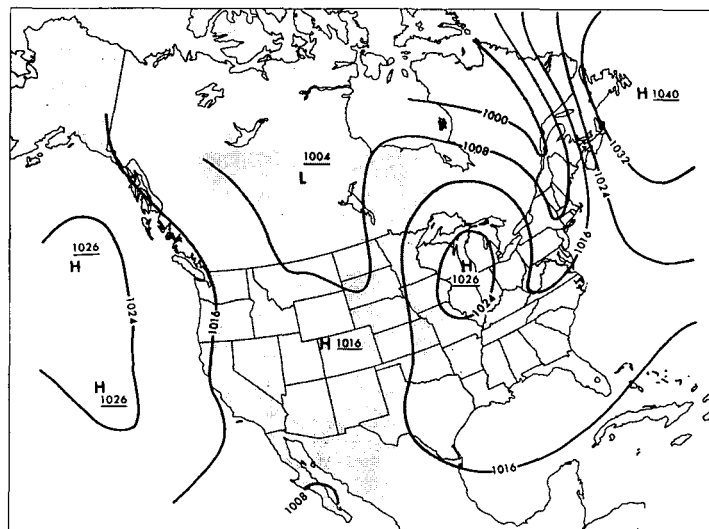


FIGURE 5.—Constant stability 24-hr. forecast of sea level pressure where $k=1.00$. Valid time is 1200 GMT, Sept. 2, 1965. Units are millibars with central values underlined.

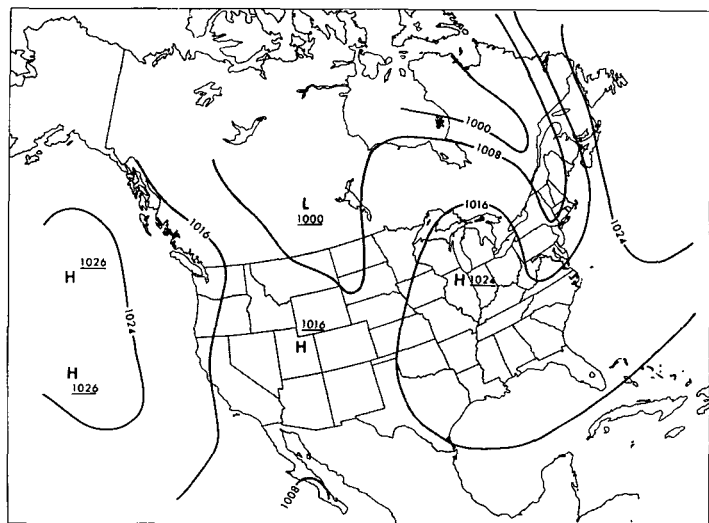


FIGURE 6.—Variable stability 24-hr. forecast of sea level pressure using k values shown in figure 4. Valid time is 1200 GMT, Sept. 2, 1965. Units are millibars with central values underlined.

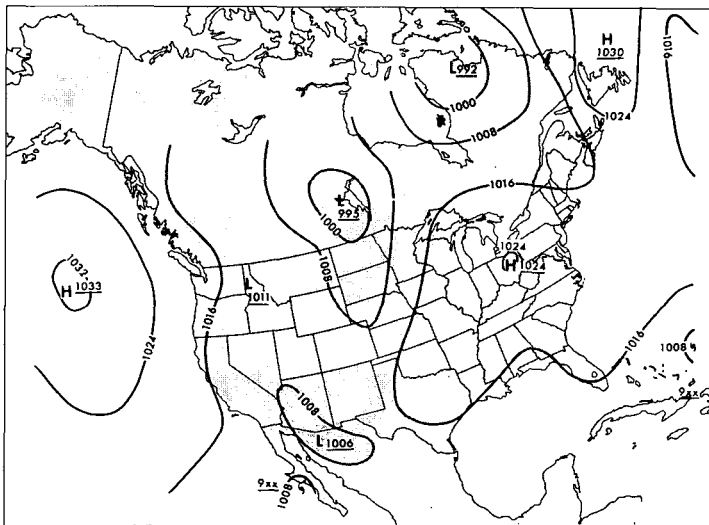


FIGURE 7.—Observed synoptic sea level pressure analysis in millibars for 1200 GMT, Sept. 2, 1965. Central values are underlined.

SECOND CASE

The second case, starting September 4, 1965 (fig. 8), shows an initial cyclone in North Dakota with a ridge of high pressure in South Central Canada ahead of the storm. The distribution of k (fig. 9) is again typical. The cyclone deepened somewhat in 24 hr. to 994 mb. (fig. 12). The variable model (fig. 11) forecast 990 mb. and the constant model prediction (fig. 10) was much too deep at 982 mb. The cyclone position forecast by the constant model was better. The ridge of high pressure remained as a ridge at about 1023 mb. The variable model forecast a 1026-mb. anticyclone while the constant model predicted a 1032-mb. anticyclone. The extreme false gradients between the two overforecast systems are very much in evidence in the constant stability product. All of the features discussed on the second case are typical and agree with the monthly average conditions.

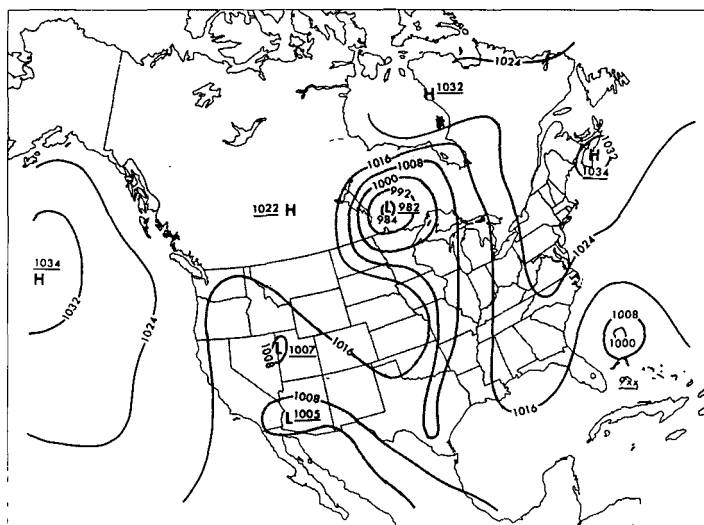


FIGURE 10.—Constant stability 24-hr. forecast of sea level pressure where $k=1.00$. Valid time is 1200 GMT, Sept. 5, 1965. Units are millibars with central values underlined.

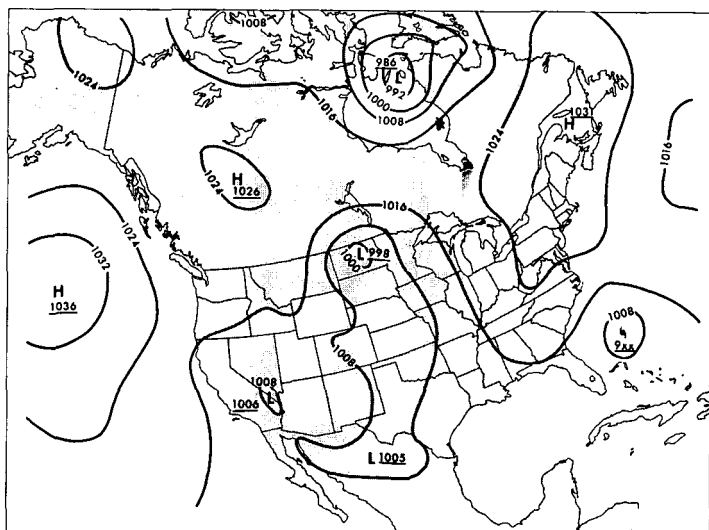


FIGURE 8.—Initial synoptic sea level pressure analysis in millibars for 1200 GMT, Sept. 4, 1965. Central values are underlined.

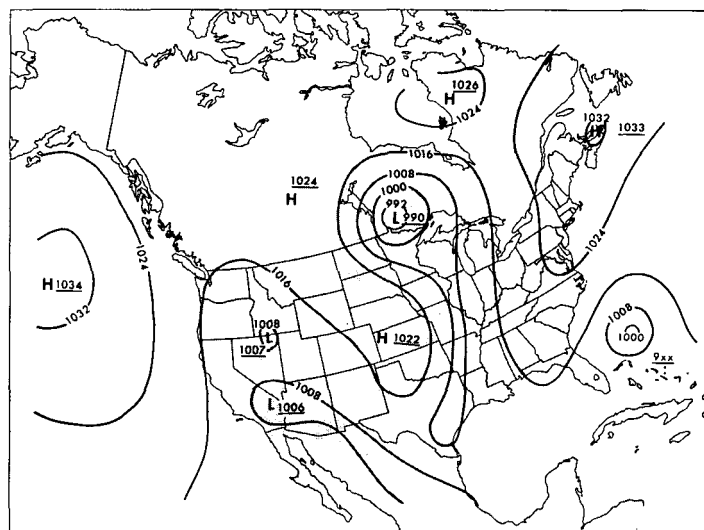


FIGURE 11.—Variable stability 24-hr. forecast of sea level pressure using k values shown in figure 9. Valid time is 1200 GMT, Sept. 5, 1965. Units are in millibars with central values underlined.

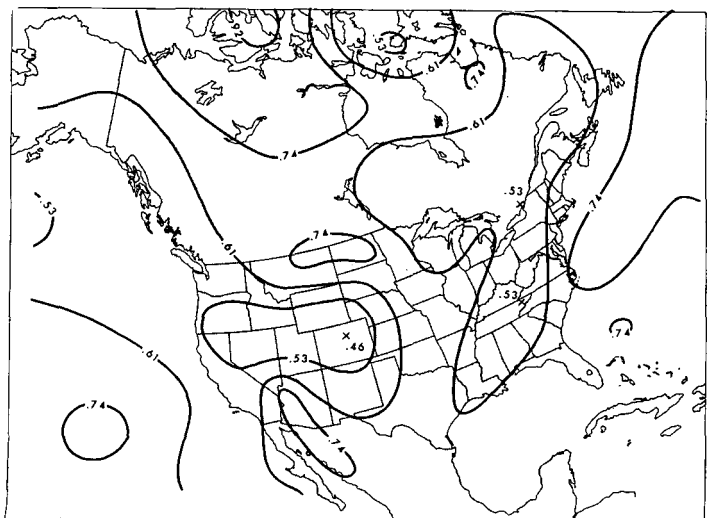


FIGURE 9.—Initial synoptic k values for 1200 GMT, Sept. 4, 1965. Low k indicates high static stability.

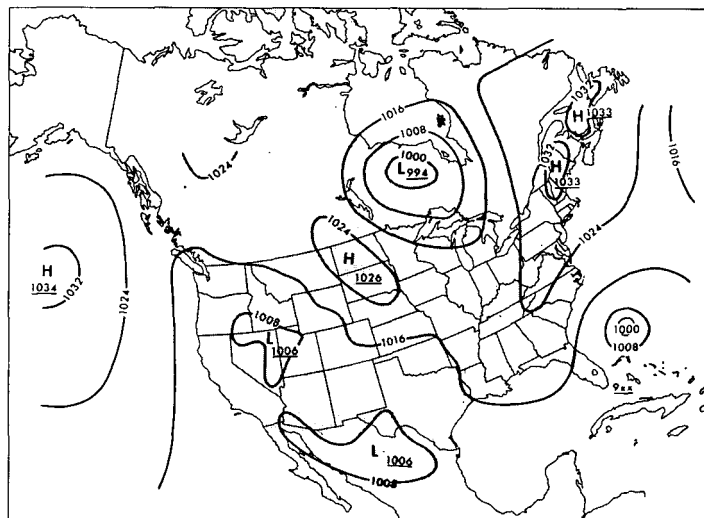


FIGURE 12.—Observed synoptic sea level pressure analysis in millibars for 1200 GMT, Sept. 5, 1965. Central values are underlined.

THIRD CASE

The September 11, 1965, initial surface analysis (fig. 13) shows two interesting features, the cyclone near the Wyoming-South Dakota border and the Great Lakes anticyclone. The k distribution (fig. 14) is normal with moderate gradients and values. The cyclone was observed (fig. 17) in 24 hr. over Nebraska. The constant stability forecast (fig. 15) and the variable stability forecast (fig. 16) produced the same central pressure error and nearly the same distance error. However, the trough of low pressure forecast toward Lake Michigan by the constant model was forecast to be a ridge of high pressure by the variable model which was more in line with the observed. The Great Lakes anticyclone intensified only 1 mb. but was forecast to intensify 3 mb. by the variable model and 6 mb. by the constant model. The position was predicted better by the variable model. Again, these features are in agreement with the average monthly characteristics.

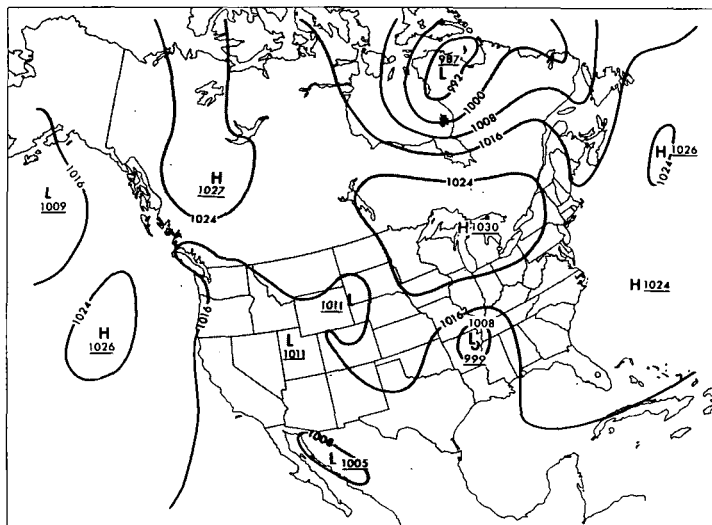


FIGURE 13.—Initial synoptic sea level pressure analysis in millibars for 1200 GMT, Sept. 11, 1965. Central values are underlined.

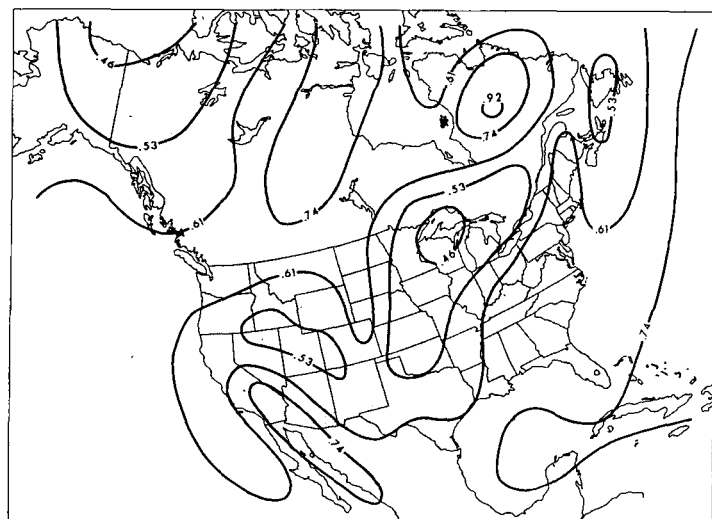


FIGURE 14.—Initial synoptic k values for 1200 GMT, Sept. 11, 1965. Low k indicates high static stability.

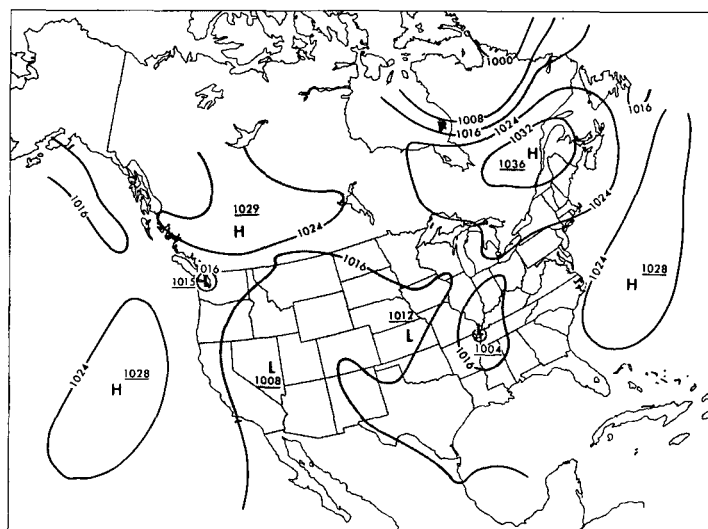


FIGURE 15.—Constant stability 24-hr. forecast of sea level pressure where $k=1.00$. Valid time is 1200 GMT, Sept. 12, 1965. Units are millibars with central values underlined.

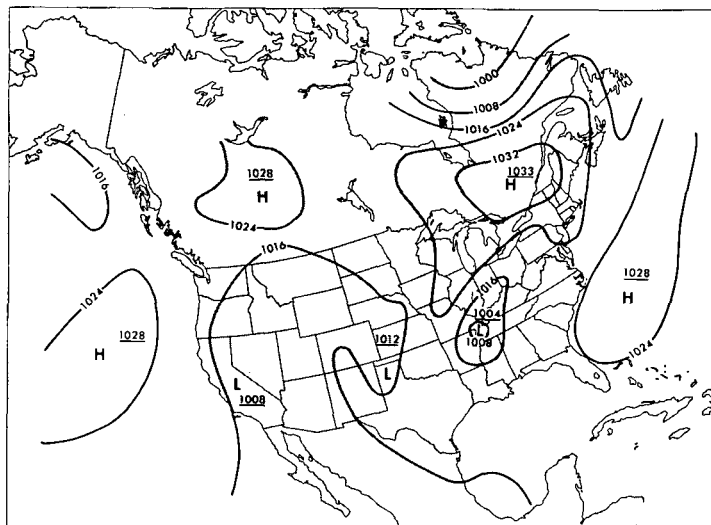


FIGURE 16.—Variable stability 24-hr. forecast of sea level pressure using k values shown in figure 14. Valid time is 1200 GMT, Sept. 12, 1965. Units are in millibars with central values underlined.

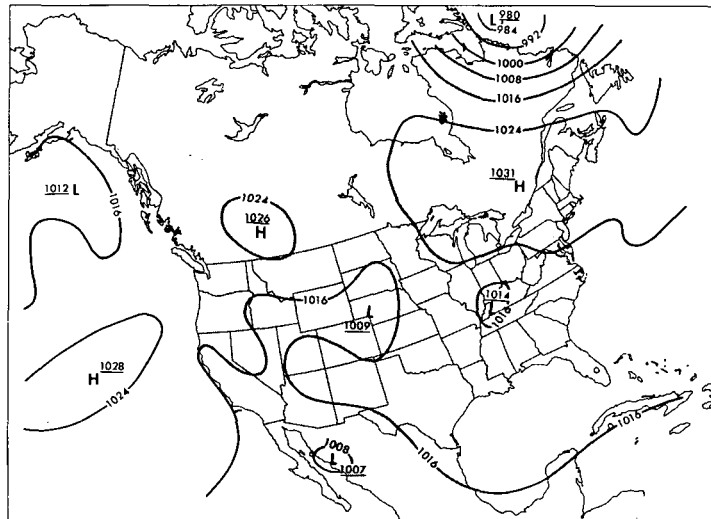


FIGURE 17.—Observed synoptic sea level pressure analysis in millibars for 1200 GMT, Sept. 12, 1965. Central values are underlined.

FOURTH CASE

The k distribution in the fourth case (fig. 19) is again as expected. The two interesting initial features (fig. 18) on September 15, 1965, are the anticyclone over Western Canada and the Great Lakes cyclone. In 24 hr. the anticyclone increased 6 mb. to 1039 mb. (fig. 22). The variable model forecast an increase of 5 mb. or 1038 mb. (fig. 21) while the constant model (fig. 20) predicted an increase of 12 mb. or 1045 mb. which is much too large. The distance error is about the same in each case. The Great Lakes cyclone moved in a normal fashion during the period and deepened a mere 1 mb. to 995 mb. The variable model forecast 994 mb. while the constant model predicted 992 mb. The position of the cyclone was forecast better by the constant model. The features discussed on the fourth case may again be considered typical and in agreement with the average conditions.

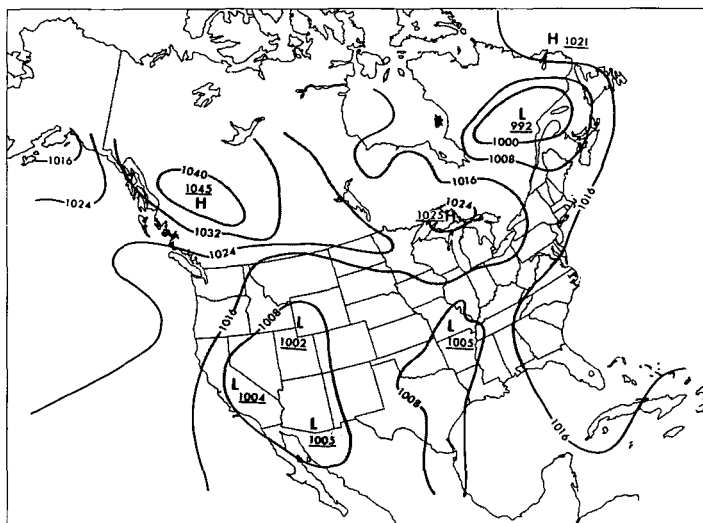


FIGURE 20.—Constant stability 24-hr. forecast of sea level pressure where $k=1.00$. Valid time is 1200 GMT, Sept. 16, 1965. Units are millibars with central values underlined.

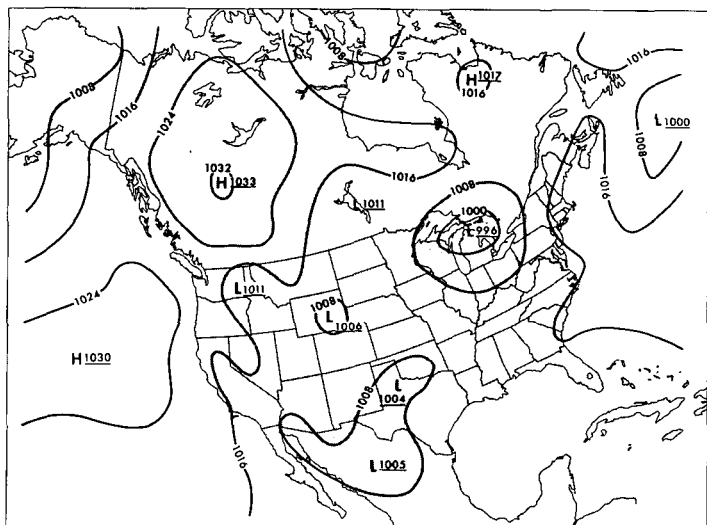


FIGURE 18.—Initial synoptic sea level pressure analysis in millibars for 1200 GMT, Sept. 15, 1965. Central values are underlined.

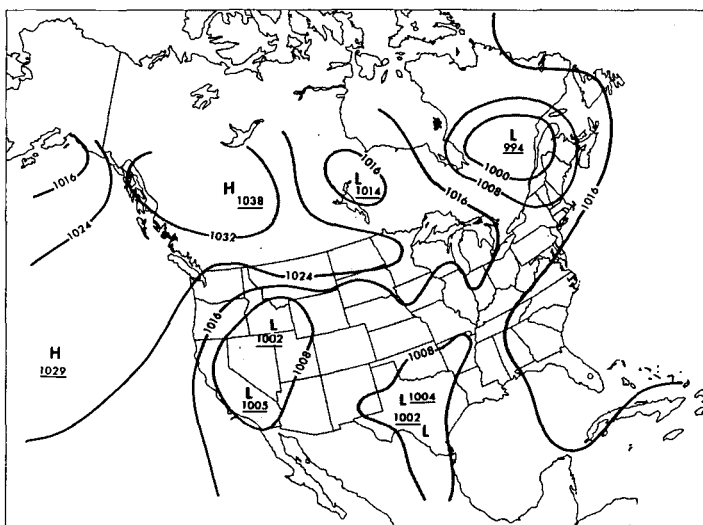


FIGURE 21.—Variable stability 24-hr. forecast of sea level pressure using k values shown in figure 19. Valid time is 1200 GMT, Sept. 16, 1965. Units are in millibars with central values underlined.

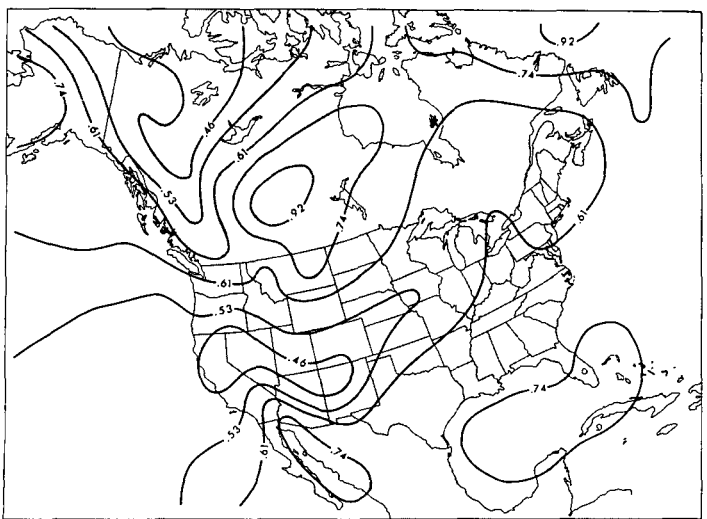


FIGURE 19.—Initial synoptic k values for 1200 GMT, Sept. 15, 1965. Low k indicates high static stability.

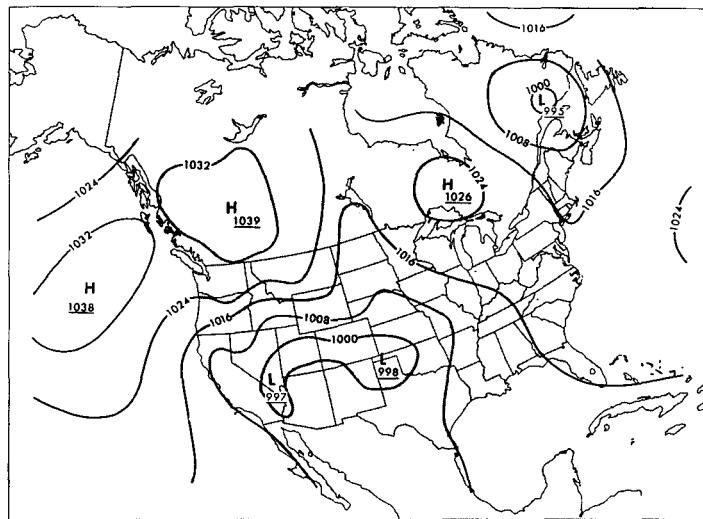


FIGURE 22.—Observed synoptic sea level pressure analysis in millibars for 1200 GMT, Sept. 16, 1965. Central values are underlined.

FIFTH CASE

Some of the greatest stability values and k gradients of the month were observed on September 17, 1965 (fig. 24). These extreme values occurred in and near the mountains and thus allowed a close look at the true effects of the weighted coefficients on cyclone position predictions. A double cyclone (fig. 23) with centers in Colorado and Arizona was located under a core of strong southwesterly winds aloft. The Colorado center moved southeastward during the forecast period to the New Mexico border (fig. 27). The variable model prediction (fig. 26) with a heavily weighted orographic term was close while the constant model (fig. 25) under the influence of the strong 500-mb. winds forecast the center to move northeastward to Nebraska. The Arizona center remained essentially stationary. The variable model again weighted the terrain strongly and forecast the center to move northward into Utah. The constant model again gave greater weight to the 500-mb. flow and predicted an east-northeastward movement to the Texas-Oklahoma Panhandle area.

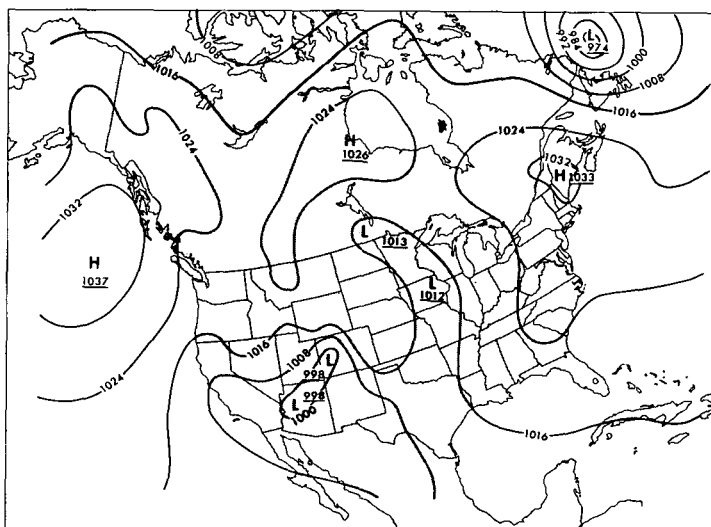


FIGURE 23.—Initial synoptic sea level pressure analysis in millibars for 1200 GMT, Sept. 17, 1965. Central values are underlined.

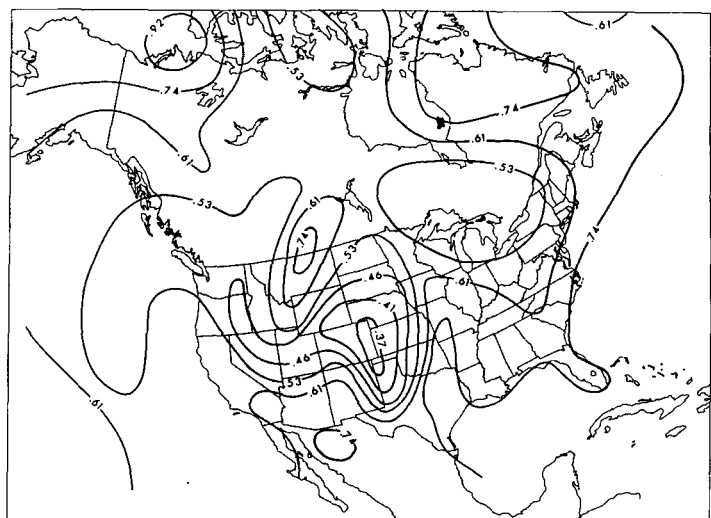


FIGURE 24.—Initial synoptic k values for 1200 GMT, Sept. 17, 1965. Low k indicates high static stability.

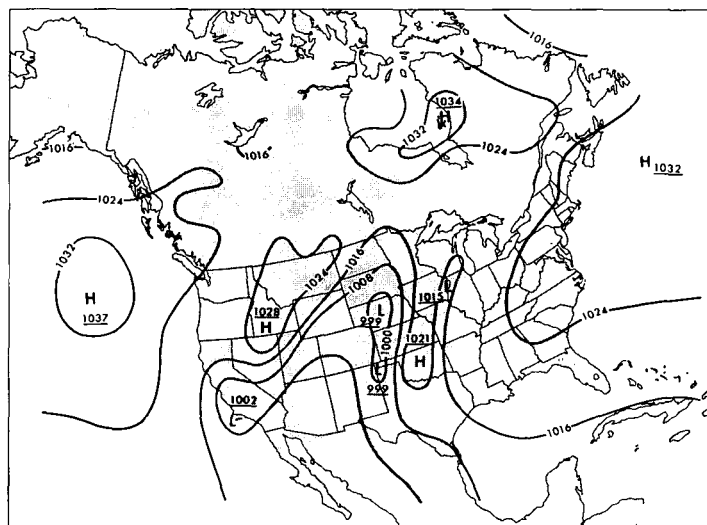


FIGURE 25.—Constant stability 24-hr. forecast of sea level pressure where $k=1.00$. Valid time is 1200 GMT, Sept. 18, 1965. Units are millibars with central values underlined.

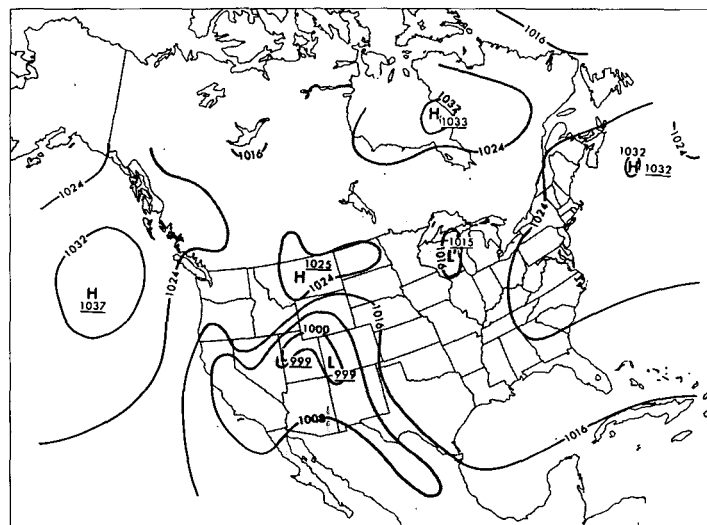


FIGURE 26.—Variable stability 24-hr. forecast of sea level pressure using k values shown in figure 24. Valid time is 1200 GMT, Sept. 18, 1965. Units are in millibars with central values underlined.

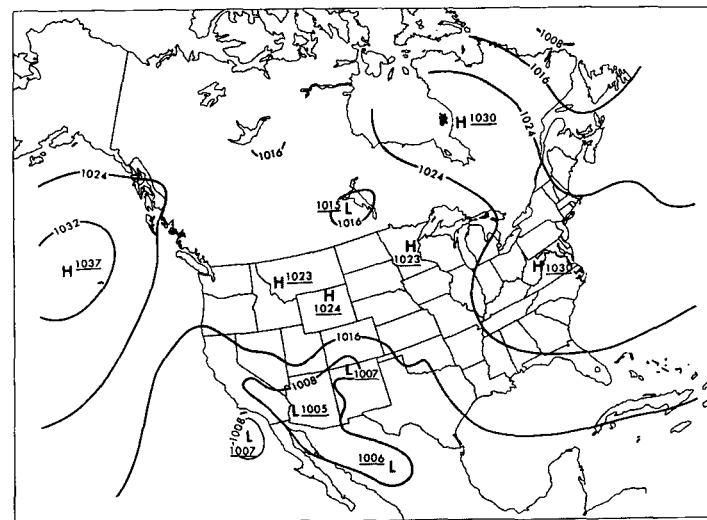


FIGURE 27.—Observed synoptic sea level pressure analysis in millibars for 1200 GMT, Sept. 18, 1965. Central values are underlined.

5. SUMMARY AND CONCLUSIONS

Significant improvements were shown by the variable stability model over the constant stability model in gradient skill score (S_1) and the central pressures of cyclones and anticyclones. These all indicate that more realistic gradients were produced by the variable stability product. Smaller improvements were shown in the distance error of anticyclones, root mean square error, and mean absolute error. The central pressures of the anticyclones and cyclones forecast by the variable stability model were slightly too high and the average gradients were also slightly too strong. Mountainous area predictions did benefit greatly by a weighted advecting mountain term.

Significant constant stability model improvement was shown only in the category of cyclone distance error. The central pressures of the anticyclones and cyclones were overpredicted as were the average pressure gradients. Speeds of both cyclones and anticyclones were faster than those shown by the variable model.

A definite improvement in the overall product can be expected by application of a variable stability model as opposed to the constant stability technique, especially in the mountainous areas and around anticyclones.

Future efforts to study the effects of variable stability in a prediction model should be computer oriented. This will not only allow the time steps to be shorter and more realistic but will allow for more complete forecast equation solution. It is not unreasonable to believe that certain terms of the forecast equations, although normally small, could under specified synoptic conditions be quite large for limited periods of time. Assumptions made for the sake of simplicity in order that the predictions could be derived graphically would no longer be required to be so restrictive. To accomplish this goal the computer efforts by Reed [17] should be expanded to include a variable stability model along the lines of the one presented here. Further refinement is probable through expansion of the Danard [3] [4] moist model concept where feed-back is possible when incorporating effects of released latent heat.

ACKNOWLEDGMENTS

We wish to thank Dr. William H. Klein, Director of the Weather Bureau's Techniques Development Laboratory, and his staff for useful suggestions. We also wish to thank the staff members, Department of Meteorology, the Pennsylvania State University, who aided in various ways.

REFERENCES

1. Air Weather Service, "Fjortoft's Graphical Method for Preparing 24 Hour 500-Mb. Prognostic Charts," *Technical Report 105-131*, Military Air Transport Service, Washington, D.C., 1955, 11 pp.
2. M. B. Danard, "On the Influence of Released Latent Heat on Cyclone Development," *Journal of Applied Meteorology*, vol. 3, No. 1, Feb. 1964, pp. 27-37.
3. M. B. Danard, "A Quasi-Geostrophic Numerical Model Incorporating Effects of Release of Latent Heat," *Journal of Applied Meteorology*, vol. 5, No. 1, Feb. 1966, pp. 85-93.
4. M. B. Danard, "Further Studies With a Quasi-Geostrophic Numerical Model Incorporating Effects of Released Latent Heat," *Journal of Applied Meteorology*, vol. 5, No. 4, Aug. 1966, pp. 388-395.
5. M. A. Estoque, "A Prediction Model for Cyclone Development Integrated by Fjortoft's Method," *Journal of Meteorology*, vol. 13, No. 2, Apr. 1956, pp. 195-202.
6. M. A. Estoque, "Graphical Integration of a Two-Level Model," *Journal of Meteorology*, vol. 14, No. 1, Feb. 1957, pp. 38-42.
7. M. A. Estoque, "A Graphically Integrable Prediction Model Incorporating Orographic Influence," *Journal of Meteorology*, vol. 14, No. 4, Aug. 1957, pp. 293-296.
8. R. Fjortoft, "On a Numerical Method of Integrating the Barotropic Vorticity Equation," *Tellus*, vol. 4, No. 3, Aug. 1952, pp. 179-194.
9. G. J. Haltiner and T. S. Hesse, "Graphical Prognosis Including Terrain Effects," *Journal of Meteorology*, vol. 15, No. 1, Feb. 1958, pp. 103-107.
10. G. J. Haltiner and Y. Wang, "Numerical Prognosis Including Non-Adiabatic Warming," *Journal of Meteorology*, vol. 17, No. 2, Apr. 1960, pp. 207-213.
11. E. C. Jarvis, "A Grid Method for Predicting the Displacement and Central Pressure of East Coast Cyclones," *Journal of Applied Meteorology*, vol. 4, No. 1, Feb. 1965, pp. 38-46.
12. D. A. Lowry, "Effects of Variable Stability in a Graphical Prediction Model," M.S. Thesis, The Pennsylvania State University, University Park, Pa., Dec. 1965, 41 pp.
13. H. S. Muench, "Evolution of a Graphical Prediction Technique Incorporating Ageostrophic Effects," *Journal of Applied Meteorology*, vol. 3, No. 5, Oct. 1964, pp. 547-553.
14. R. J. Reed, "A Graphical Method for Preparing 1000-Millibar Prognostic Charts," *Journal of Meteorology*, vol. 14, No. 1, Feb. 1957, pp. 65-70.
15. R. J. Reed, "A Graphical Prediction Model Incorporating a Form of Nonadiabatic Heating," *Journal of Meteorology*, vol. 15, No. 1, Feb. 1958, pp. 1-8.
16. R. J. Reed, "On the Practical Use of Graphical Prediction Methods," *Monthly Weather Review*, vol. 88, No. 6, June 1960, pp. 209-218.
17. R. J. Reed, "Experiments in 1000-Mb. Prognosis," *National Meteorological Center Technical Memorandum No. 26*, U.S. Weather Bureau, Washington, D.C., 1963, 42 pp.
18. J. S. Sawyer and F. H. Bushby, "A Baroclinic Model Suitable for Numerical Integration," *Journal of Meteorology*, vol. 10, No. 1, Feb. 1953, pp. 54-59.
19. S. Teweles, Jr., and H. B. Wobus, "Verification of Prognostic Charts," *Bulletin of the American Meteorological Society*, vol. 35, No. 10, Dec. 1954, pp. 455-463.
20. K. W. Veigas and F. P. Ostby, Jr., "Application of a Moving Coordinate Prediction Model to East Coast Cyclones," *Journal of Applied Meteorology*, vol. 2, No. 1, Feb. 1963, pp. 24-38.

[Received April 26, 1967; revised September 11, 1967]